

# Diagnosis of Planar Arrays through Phaseless Measurements and Sparsity Promotion

R. Palmeri, T. Isernia, and A. F. Morabito

**Abstract**—A new Compressive-Sensing-inspired approach is proposed to the detection of faulty radiators in planar antenna arrays from a reduced set of phaseless far-field measurements. In order to deal with whatever kind of arrays, the problem is cast as the recovery of the aperture-field distribution, and two new convex-programming solution procedures are introduced. The first one relies on an improvement of the Total Variation norm technique, while the second one exploits a new aperture field expansion which allows drastically reducing the number of unknowns of the problem. A wide set of numerical experiments involving benchmark scenarios as well as full-wave data relative to a realistic antenna is provided in support of the given theory.

**Index Terms**—Antenna arrays, compressed sensing, fault diagnosis.

## I. INTRODUCTION

IN recent years, the problem of detecting and localizing the failures in given Arrays Under Test (AUTs) has stimulated researchers to develop new strategies allowing to address the requirements of the emerging technologies [1]-[13]. Amongst the introduced approaches, the ones based on far-field measurements are of large interest as they allow monitoring AUTs often located in non-directly accessible areas and can also exploit the Compressive Sensing (CS) [14] theory.

CS is usually exploited in array synthesis to minimize the number of elements for fixed radiation performances [15]-[21]. In array diagnosis, it can be used to minimize the number of measurements (say  $M$ ) such to guarantee an accurate detection and localization of faulty elements. Notably, while being supposed to be larger than the number of faulty elements (say  $S$ ),  $M$  can be anyway much lower than the number of elements of the AUT (say  $N$ ) [1]-[8].

As well known, CS theory is developed and well assessed for the case of *linear* problems which, in array diagnosis applications, translates into the requirement of measuring both the *amplitude and phase* of the field [1]-[6]. However, for the case of 1-D arrays whose far field distribution can be written in terms of the array factor (referred in the following as ‘ideal’ AUTs), an innovative CS-inspired technique has been introduced in [8] in order to solve the diagnosis problem by

means of *phaseless* far-field measurements. In particular, it has been shown that, provided that the percentage of faulty elements is low and a smart measurement strategy is used, the pertaining non-linear problem can be solved as a CS-based Convex Programming (CP) one. Also, it has been proved that an accurate faults detection can be achieved provided that  $M \geq 8S$ , which agrees with the rule of thumb  $M \geq 4S$  determined in [1] for the case of *amplitude and phase* measurements.

In this letter, by keeping the assumption of phaseless measurements, the 1-D method introduced by [8] is extended to the ON-OFF diagnosis of 2-D AUTs. In particular, we first deal with planar ideal AUTs (Section II), and then we propose a new technique for the diagnosis of any kind of 2-D AUTs having whatever layout and radiating elements (Section III).

In the following, after having presented the proposed approach in Sections II and III, in Section IV we check its actual performances through a large set of numerical experiments (including CST full-wave simulations of benchmark realistic arrays in the presence of mutual coupling and mounting-platform effects). Conclusions follow.

## II. THE CASE OF IDEAL ARRAYS

Let us suppose dealing with a 2-D AUT composed, according to a square equispaced grid, of  $N_x$  elements (with a spacing equal to  $d_x$ ) along the  $x$ -axis and  $N_y$  elements (with a spacing equal to  $d_y$ ) along the  $y$ -axis. Such an antenna will be referred in the following as ‘gold’ AUT provided that all of its elements are correctly operating, while it will be referred as ‘faulty’ AUT in case  $S$  of its elements are not working (i.e., exhibit a null excitation). Moreover, by keeping the usual assumption (as done in [1],[2],[5],[8]) that the AUT far field is given by the array factor, and denoting with  $I_{pq}$  the excitation of the element located at the intersection between the  $p$ -th row and the  $q$ -th column of the layout, the fields respectively radiated by the gold and faulty AUTs can be written as:

$$E^G(u, v) = \sum_{p=1}^{N_x} \sum_{q=1}^{N_y} I_{pq}^G e^{j(pu+qv)} \quad (1.a)$$

$$E^F(u, v) = \sum_{p=1}^{N_x} \sum_{q=1}^{N_y} I_{pq}^F e^{j(pu+qv)} \quad (1.b)$$

where the apexes  $G$  and  $F$  stand for “gold” and “faulty”,

This is the post-print of the following article: R. Palmeri, T. Isernia, and A. F. Morabito, “Diagnosis of Planar Arrays through Phaseless Measurements and Sparsity Promotion,” IEEE Antennas and Wireless Propagation Letters, vol. 18, n. 6, pp. 1273 - 1277, 2019. Article has been published in final form at: <https://ieeexplore.ieee.org/document/8704892>. DOI: 10.1109/LAWP.2019.2914529.

1536-1225 © [2019] IEEE. Personal use of this material is permitted. Permission from IEEE must be obtained for all other uses, in any current or future media, including reprinting/republishing this material for advertising or promotional purposes, creating new collective works, for resale or redistribution to servers or lists, or reuse of any copyrighted component of this work in other works.”

$\beta = 2\pi/\lambda$  ( $\lambda$  being the wavelength),  $u = \beta d_x \sin\theta \cos\phi$ , and  $v = \beta d_y \sin\theta \sin\phi$  ( $\theta$  and  $\phi$  respectively denoting the usual elevation and azimuth angles).

Then, by considering the *differential* field:

$$\Delta E(u, v) = E^G(u, v) - E^F(u, v) = \sum_{p=1}^{N_x} \sum_{q=1}^{N_y} \Delta I_{pq} e^{j(pu+qv)} \quad (2)$$

with  $\Delta I_{pq} = I_{pq}^G - I_{pq}^F$ , in a generic point  $(u_m, v_m)$  the following relation will hold true:

$$|E^F(u_m, v_m)|^2 - |E^G(u_m, v_m)|^2 = |\Delta E(u_m, v_m)|^2 + \alpha_m \quad (3.a)$$

$$\alpha_m = -2\text{Re}\langle E^G(u_m, v_m), \Delta E(u_m, v_m) \rangle \quad (3.b)$$

Notably, the differential field and the corresponding excitations are sparse as long as  $S \ll N$ . Therefore, by introducing the real vector  $\boldsymbol{\tau} = [\tau_1, \tau_2, \dots, \tau_N]$  (with  $N = N_x N_y$ )<sup>1</sup>, the problem of determining  $\Delta I_{pq} \forall (p, q)$  (i.e., the number and location of faulty elements) starting only from the knowledge of  $|E^F|^2$  and the gold AUT can be solved through the same approach as in [8], i.e.:

$$\min_{\tau_1, \tau_2, \dots, \tau_N} \|\mathbf{1} - \boldsymbol{\tau}\|_1 \quad (4.a)$$

subject to:

$$\|\boldsymbol{\rho}\|_2 < \varepsilon \quad (4.b)$$

$$I_n^F = \tau_n I_n^G \text{ for } n = 1, \dots, N \quad (4.c)$$

$$0 \leq \tau_n \leq 1 \text{ for } n = 1, \dots, N \quad (4.d)$$

being  $\boldsymbol{\rho} = [\rho_1, \rho_2, \dots, \rho_M]$ , with:

$$\rho_m = \frac{|E^F(u_m, v_m)|^2 - |E^G(u_m, v_m)|^2 - \alpha_m - |\Delta E(u_m, v_m)|^2}{|E^G(u_m, v_m)|^2} \quad (4.e)$$

In fact, by the virtue of (4.c), it will result  $\Delta I_n = I_n^G(1 - \tau_n) \forall n$  and hence if  $\Delta \mathbf{I}$  is sparse then  $(\mathbf{1} - \boldsymbol{\tau})$  is sparse as well, so that CS can be profitably applied. In particular, the minimization of functional (4.a) is meant to enforce sparsity, while conditions (4.b) ensures the fulfillment of the (normalized) data equations (3) within a given tolerance  $\varepsilon$ .

Notably, as long as  $S \ll N$ , the quadratic term in (3.a) and (4.e), i.e.,  $|\Delta E|^2$ , will be small<sup>2</sup> with respect to  $\alpha_m$  and hence, due to the linearity of constraints (4.c) and (4.d), the problem (4) results in a CP one, with the inherent advantages.

The proposed approach exhibits a decisive advantage with respect to all techniques resorting to amplitude and phase measurements (e.g., [1]-[6]). In fact, it does not require an

<sup>1</sup> As long as one deals with the ON-OFF diagnosis, the introduction of  $\boldsymbol{\tau}$  allows halving the number of unknowns of the problem with respect to the cases wherein the complex vector  $\mathbf{I}^F$  is directly looked for [8].

<sup>2</sup> A further lowering of the weight of  $|\Delta E|^2$  can be achieved by performing the measurements in those points where  $E^G$  has a large intensity.

accurate phase measurement (i.e., a stable phase reference and an accurate positioning of the probes in the order of a small fraction of  $\lambda$ ) and hence provides a relevant simplification of the overall diagnosis. Moreover, formulation (4) is quite general and lends itself to the extension to whatever kind of planar arrays (including realistic arrays wherein mutual coupling and mounting-platform effects are present), which is the subject of the following Section.

### III. THE CASE OF REALISTIC ARRAYS

Dealing with the diagnosis of realistic planar arrays (for which the radiation pattern is different from the array factor, or the array factor cannot even be defined) is possible by determining the aperture field distribution (rather than the excitations) associated to the faulty AUT. This has been done in [3] and [11] which, however, solved the diagnosis problem by exploiting *amplitude and phase* measurements.

In order to apply the approach presented in Section II to realistic AUTs, we keep the problem formulation (4) by replacing the far-field expressions (1) with the following ones:

$$\mathbf{E}^G(u, v) = \int \mathbf{E}_{ap}^G(x, y) e^{j(ux+vy)} dx dy \quad (5.a)$$

$$\mathbf{E}^F(u, v) = \int \mathbf{E}_{ap}^F(x, y) e^{j(ux+vy)} dx dy \quad (5.b)$$

where  $\mathbf{E}_{ap}^G(x, y) = E_{ap_x}^G(x, y)\hat{x} + E_{ap_y}^G(x, y)\hat{y}$  and  $\mathbf{E}_{ap}^F(x, y) = E_{ap_x}^F(x, y)\hat{x} + E_{ap_y}^F(x, y)\hat{y}$  respectively are the tangential fields on the gold and faulty AUTs' aperture<sup>3</sup>. Accordingly, the  $\Delta \mathbf{I}$  vector relative to (2) is now replaced by  $\Delta \mathbf{E}_{ap} = \mathbf{E}_{ap}^G - \mathbf{E}_{ap}^F$ .

Effective solution procedures relying on (5) are presented in the two following Subsections.

#### A. Improved Total-Variation norm

Since the aperture field is a continuous distribution, in the formulation (5) the sparsity of the new unknown  $\Delta \mathbf{E}_{ap} = [\Delta \mathbf{E}_{ap_1}, \dots, \Delta \mathbf{E}_{ap_{N_p}}]$  ( $N_p$  denoting the number of sampling points in the  $xy$ -plane) may be compromised. To counteract this issue, by taking advantage of the fact that  $\Delta \mathbf{E}_{ap}$  is expected to resemble a piecewise-constant distribution, we solve the problem as a total-variation (TV) [22] norm-minimization one. This has been done also in [3] (wherein amplitude and phase measurements are exploited) but here, encouraged by the good results in inverse scattering problems [23], also the derivatives along the principal and secondary diagonals  $x = \pm y$  are considered. In fact, through the arising modified TV-norm it is possible to counteract the resolution

<sup>3</sup> For the same reasons as the ones discussed in [8], Fourier relationships such as (5) guarantee a low mutual coherence between the sensing and representation basis and hence allow a successful application of the CS theory.

losses due to lack of phase information and hence achieve a better regularization of the problem at hand.

Accordingly, by denoting with  $\mathbf{D}_h\Delta\mathbf{E}_{ap}$ ,  $\mathbf{D}_v\Delta\mathbf{E}_{ap}$ ,  $\mathbf{D}_d^+\Delta\mathbf{E}_{ap}$ , and  $\mathbf{D}_d^-\Delta\mathbf{E}_{ap}$  the vectors containing the forward differences of  $\Delta\mathbf{E}_{ap}$  along the horizontal, vertical, principal-diagonal, and secondary-diagonal directions, respectively, the optimization problem (4) can be recast as follows:

$$\min_{\Delta\mathbf{E}_{ap_1}, \dots, \Delta\mathbf{E}_{ap_{N_p}}} \left\{ \|\mathbf{D}_h\Delta\mathbf{E}_{ap}\|_1 + \|\mathbf{D}_v\Delta\mathbf{E}_{ap}\|_1 + \|\mathbf{D}_d^+\Delta\mathbf{E}_{ap}\|_1 + \|\mathbf{D}_d^-\Delta\mathbf{E}_{ap}\|_1 \right\} \quad (6.a)$$

subject to:

$$\|\boldsymbol{\rho}\|_2 < \varepsilon \quad (6.b)$$

wherein  $\boldsymbol{\rho}$  is defined as in (4.e) by replacing (1) by using (5).

### B. The Active Element Aperture Pattern adoption

As it can be understood from (6), in case of aperiodic or realistic arrays having a number of degrees of freedom [24] larger than the number of elements, the new formulation of the problem entails an increase of the number of unknowns (from  $N$  to  $N_p$ ). This limitation, which may lead to high computational times in case of electrically-large arrays, can be overcome by extending the adoption of the original ‘active element pattern’ concept [25] to the case of the aperture field. By so doing, and denoting with  $c_1, c_2, \dots, c_N$  arbitrary coefficients, the following representation can be introduced:

$$\mathbf{E}_{ap}(x, y) = \sum_{n=1}^N c_n \mathbf{AA}F_n(x, y) \quad (7)$$

In the expansion (7), which is never been used before, we named ‘ $n$ -th Active-element Aperture Field’ ( $\mathbf{AA}F_n$ ) the aperture field generated by the AUT when its  $n$ -th antenna has a unitary excitation while all the other antennas are OFF.

Then, by considering expansion (7) for the gold and faulty AUTs, the differential aperture field can be represented as:

$$\Delta\mathbf{E}_{ap}(x, y) = \sum_{n=1}^N \Delta c_n \mathbf{AA}F_n(x, y) \quad (8)$$

(with  $\Delta c_n = c_n^G - c_n^F \forall n$ ) and the problem can be recast as:

$$\min_{\Delta c_1, \Delta c_2, \dots, \Delta c_N} \|\Delta\mathbf{c}\|_1 \quad (9.a)$$

subject to:

$$\|\boldsymbol{\rho}\|_2 < \varepsilon \quad (9.b)$$

wherein  $\Delta\mathbf{c} = [\Delta c_1, \Delta c_2, \dots, \Delta c_N]$  and the expansion (8) are used.

Notably, whatever the AUT at hand, the new representation allows solving the problem in terms of  $N$  unknowns, i.e., as in problem (4) but working, this time, also in case of realistic AUTs. In particular, with respect to the case of ideal AUTs, the only additional task will be a pre-processing step devoted to the  $\mathbf{AA}F$  offline computation.

## IV. NUMERICAL ASSESSMENT

We tested the proposed approaches in both cases of ideal and realistic AUTs. The results relative to the two cases are separately discussed in the two following Subsections.

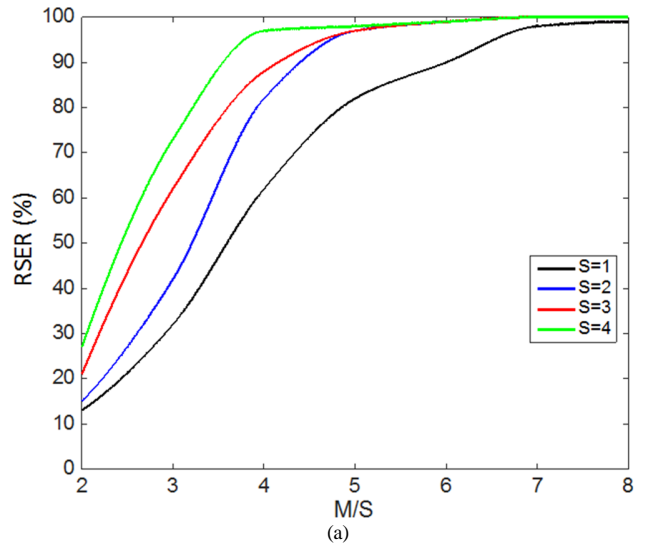
### A. Ideal AUTs

We used as AUT a square array with  $N_x = N_y = 5$  and  $d_x = d_y = 0.5\lambda$  with complex random excitations. We considered different pairs  $(S, M)$  and, for each instance, we solved 100 times problem (4) (with  $\varepsilon = 0.001$ ) and evaluated the normalized mean square error (NMSE), i.e.,

$$NMSE = \frac{\|\Delta\mathbf{I} - \widehat{\Delta\mathbf{I}}\|_2^2}{\|\Delta\mathbf{I}\|_2^2} \quad (10)$$

( $\Delta\mathbf{I}$  and  $\widehat{\Delta\mathbf{I}}$  denoting the vectors containing the actual and retrieved differential excitations, respectively). Then, we determined the rate of success recovery (RSER) by assuming ‘successful’ any simulation leading to  $NMSE \leq 0.01$ . The  $M$  measurement locations have been randomly chosen amongst those sampling points wherein the far field of the gold AUT attained a normalized amplitude higher than -20dB.

Fig. 1 reports the achieved RSER as a function of the ratio  $M/S$  in both cases of noise-free and noisy (SNR=30dB) data. As it can be seen, the conditions  $M \geq 6S$  and  $M \geq 7S$  respectively entail a probability of success of at least 90% (noise-free data) and 80% (noisy data). Moreover, for  $S > 1$  and noise-free data,  $M \geq 5S$  brought a probability of success larger than 95%. Besides confirming the high reliability of the proposed technique, these results reveal a reduction of  $M$  (for equal RSER values) with respect to the 1-D case dealt with in [8]<sup>4</sup>.



<sup>4</sup> The improvement of performances with respect to the 1-D case can also be attributed to the lack of ‘zero-flipping based’ [27]-[29] multiple solutions.

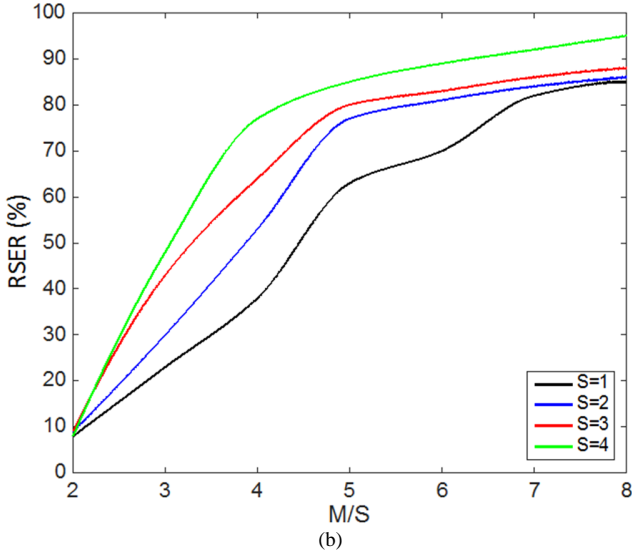


Fig. 1. Ideal AUTs: RSER achieved in case of noiseless (a) and noisy (b) data.

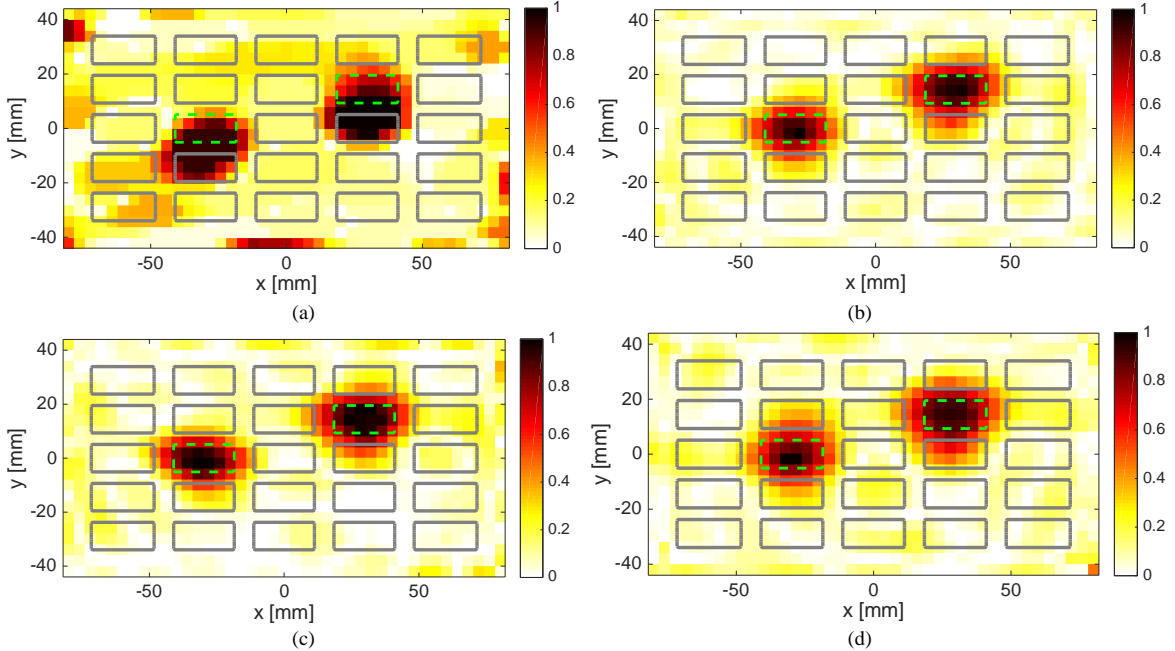


Fig. 2.  $|\widehat{\Delta E}_{ap}|$  achieved through the improved TV-norm approach for different measurement configurations: (a)  $M = 72$  phaseless data; (b)  $\widehat{M} = 30$  complex and  $M = 90$  phaseless data; (c)  $\widehat{M} = 15$  and  $M = 75$ ; (d)  $\widehat{M} = 10$  and  $M = 50$ . Faulty elements contoured in green color.

### B. Realistic AUTs

We considered  $N_x = N_y = 5$  and the same radiating element and inter-element spacing as in [3]. The AUT has  $d_x = \lambda$ ,  $d_y = 0.5\lambda$ , and is composed of WR90 open-ended waveguides working at 10 GHz and having a size of  $22.86 \times 10.16$  mm<sup>2</sup> as dictated by [26]. All fields have been calculated through CST Microwave Studio full-wave simulations. In particular, the waveguides have been excited in such a way that only the fundamental mode propagates and the diagnosis has been aimed at retrieve the  $E_{ap,y}^F$  distribution at a  $\lambda/6$  distance from the AUT. The NMSE has been calculated as:

$$NMSE_{ap} = \frac{\|\Delta E_{ap} - \widehat{\Delta E}_{ap}\|_2^2}{\|\Delta E_{ap}\|_2^2} \quad (11)$$

wherein  $\Delta E_{ap}$  and  $\widehat{\Delta E}_{ap}$  are the vectors containing the actual and retrieved differential aperture fields, respectively.

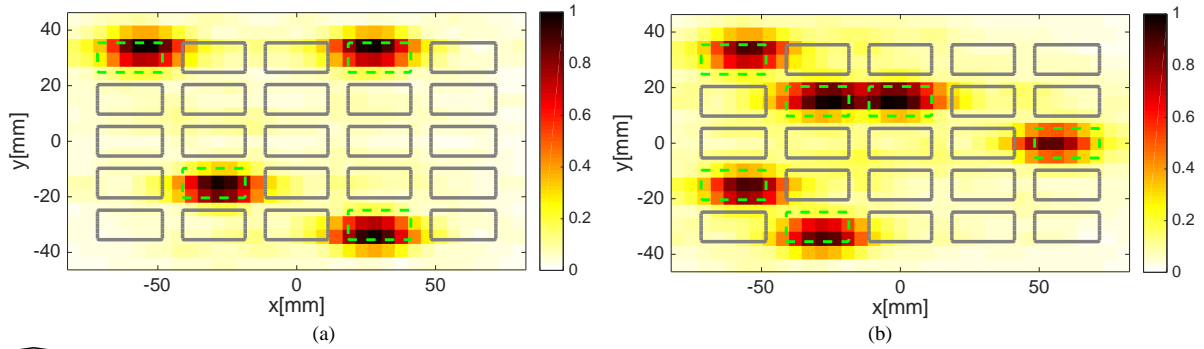


Fig. 3.  $|\widehat{\Delta E_{ao}}|$  provided by the AAF approach for  $M = 4S$  phaseless measurements with (a)  $S = 4$  and (b)  $S = 6$ . Faulty elements contoured in green color.

Fully-satisfactory results have been achieved by exploiting measurements of just the  $\phi$ -component of the far field.

Fig. 2 reports the outcomes of the modified TV-norm approach presented in Section III.A. In particular, subplot (a) shows the results achieved for  $S = 2$  and  $M = 72$  phaseless measurements ( $NMSE_{ap} = 0.04$  for  $\varepsilon = 0.1$ ), while subplots (b)-(d) refers to a hybrid measurement configuration given by  $\widehat{M}$  complex plus  $M$  phaseless far-field measurements. The results achieved for different values of  $\widehat{M}$  and  $M$  are summarized in Tab. 1. Notably, the approach allowed achieving fully-satisfactory results by exploiting a number of measurements significantly lower than the Nyquist one. In fact, since the AUT covers a  $15\lambda^2$  area, the number of independent square-amplitude samples is equal to 240 [24].

A more accurate diagnosis by exploiting an even lower number of measurements has been possible by exploiting the AAF approach. In particular, by setting  $M = 4S$  and  $\varepsilon = 0.001$ , we achieved  $NMSE_{ap} = 1.1 \cdot 10^{-8}$  for  $S = 4$  and  $NMSE_{ap} = 3.5 \cdot 10^{-9}$  for  $S = 6$  (see Fig. 3). For these test cases, the computational time resulted lower than 10s (while several minutes were required by the TV-norm approach).

## V. CONCLUSIONS

A new approach to the diagnosis of planar arrays has been presented and assessed. Differently from a large body of literature, all the proposed solution procedures rely only on phaseless measurements. Despite the consequent non-linearity of the problem, new tools and field representations has been introduced in such a way to take maximum advantage of the CS theory and improve the computational efficiency with respect to the state-of-the-art approaches.

$M$	$\widehat{M}$	$NMSE_{ap}$
72	0	0.044
90	30	0.015
75	15	0.017

Tab.1. Summary of the results achieved by the improved TV-norm approach.

## REFERENCES

- [1] M. D. Migliore, "Array diagnosis from far-field data using the theory of random partial Fourier matrices," *IEEE Antennas and Wireless Propagation Letters*, vol. 12, pp. 745-748, 2013.
- [2] W. Li, W. Deng, and M. D. Migliore, "A deterministic far-field sampling strategy for array diagnosis using sparse recovery," *IEEE Antennas and Wireless Propagation Letters*, vol. 17, n. 7, pp. 1261-1265, 2018.
- [3] B. Fuchs, L. Le Coq, and M. D. Migliore, "Fast antenna array diagnosis from a small number of far-field measurements," *IEEE Transactions on Antennas and Propagation*, vol. 64, n. 6, pp. 2227-2235, 2016.
- [4] M. Salucci, A. Gelmini, G. Oliveri, and A. Massa, "Planar arrays diagnosis by means of an advanced bayesian compressive processing," *IEEE Transactions on Antennas and Propagation*, vol. 66, n. 11, pp. 5892-5906, 2018.
- [5] G. Oliveri, P. Rocca, and A. Massa, "Reliable diagnosis of large linear arrays: a bayesian compressive sensing approach," *IEEE Transactions on Antennas and Propagation*, vol. 60, n. 10, pp. 4627-4636, 2012.
- [6] Y. Zhang and H. Zhao, "Failure diagnosis of a uniform linear array in the presence of mutual coupling," *IEEE Antennas and Wireless Propagation Letters*, vol. 14, pp. 1010-1013, 2015.
- [7] B. Fuchs and L. Le Coq, "Excitation retrieval of microwave linear arrays from phaseless far-field data," *IEEE Transactions on Antennas and Propagation*, vol. 63, n. 2, pp. 748-754, 2015.
- [8] A. F. Morabito, R. Palmeri, and T. Isernia, "A compressive-sensing-inspired procedure for array antenna diagnostics by a small number of phaseless measurements," *IEEE Transactions on Antennas and Propagation*, vol. 64, n. 7, pp. 3260-3265, 2016.
- [9] M. D. Migliore, S. Costanzo, A. Borgia, D. Pinchera, and G. Di Massa, "Failures identification in a linear slot array using a sparse recovery technique," *Proceedings of the 8th European Conference on Antennas and Propagation*, pp. 3214-3215, The Hague, The Netherlands, on 6-11 April 2014.
- [10] S. Costanzo, A. Borgia, G. Di Massa, D. Pinchera, and M. D. Migliore, "Radar array diagnosis from undersampled data using a compressed sensing/sparse recovery technique," *Journal of Electrical and Computer Engineering*, vol. 2013, Article ID 627410, 5 pages, 2013.
- [11] G. Di Massa and S. Costanzo, "Fast diagnostics of conformal arrays," *WorldCIST*, vol. 2, pp. 1494-1501, 2018.
- [12] S. Costanzo and G. Di Massa, "Spatial domain indirect holographic technique for antenna near-field phaseless measurements," *Radio Science*, vol. 52, n. 4, pp. 432-438, 2017.
- [13] M. D. Migliore, "A compressed sensing approach for array diagnosis from a small set of near-field measurements," *IEEE Transactions on Antennas and Propagation*, vol. 59, n. 6, pp. 2127-2133, 2011.

This is the post-print of the following article: R. Palmeri, T. Isernia, and A. F. Morabito, "Diagnosis of Planar Arrays through Phaseless Measurements and Sparsity Promotion," *IEEE Antennas and Wireless Propagation Letters*, vol. 18, n. 6, pp. 1273 - 1277, 2019. Article has been published in final form at: <https://ieeexplore.ieee.org/document/8704892>. DOI: 10.1109/LAWP.2019.2914529.

1536-1225 © [2019] IEEE. Personal use of this material is permitted. Permission from IEEE must be obtained for all other uses, in any current or future media, including reprinting/republishing this material for advertising or promotional purposes, creating new collective works, for resale or redistribution to servers or lists, or reuse of any copyrighted component of this work in other works."

- [14] E. J. Candès, J. K. Romberg, and T. Tao, "Robust uncertainty principles: exact signal reconstruction from highly incomplete frequency information," *IEEE Transactions on Information Theory*, vol. 52, n. 2, pp. 489-509, 2006.
- [15] A. F. Morabito, and P. Rocca, "Reducing the number of elements in phase-only reconfigurable arrays generating sum and difference patterns," *IEEE Antennas and Wireless Propagation Letters*, vol. 14, pp. 1338-1341, 2015.
- [16] G. Oliveri and A. Massa, "Bayesian compressive sampling for pattern synthesis with maximally sparse non-uniform linear arrays," *IEEE Transactions on Antennas and Propagation*, vol. 59, n. 2, pp. 467-481, 2011.
- [17] G. Oliveri, M. Carlin, and A. Massa, "Complex-weight sparse linear array synthesis by Bayesian Compressive Sampling," *IEEE Transactions on Antennas and Propagation*, vol. 60, n. 5, pp. 2309-2326, 2012.
- [18] G. Prisco and M. D'Urso, "Maximally sparse arrays via sequential convex optimizations," *IEEE Antennas and Wireless Propagation Letters*, vol. 11, pp. 192-195, 2012.
- [19] A. F. Morabito, "Synthesis of maximum-efficiency beam arrays via convex programming and compressive sensing," *IEEE Antennas and Wireless Propagation Letters*, vol. 16, pp. 2404-2407, 2017.
- [20] B. Fuchs, "Synthesis of sparse arrays with focused or shaped beam pattern via sequential convex optimizations," *IEEE Transactions on Antennas and Propagation*, vol. 60, n. 7, pp. 3499-3503, 2012.
- [21] A. F. Morabito, A. R. Laganà, G. Sorbello, and T. Isernia, "Mask-constrained power synthesis of maximally sparse linear arrays through a compressive-sensing-driven strategy," *Journal of Electromagnetic Waves and Applications*, vol. 29, n. 10, pp. 1384-1396, 2015.
- [22] P. Blomgren and T. F. Chan, "Color TV: total variation methods for restoration of vector-valued images," *IEEE Transactions on Image Processing*, vol. 7, n. 3, pp. 304-309, 1998.
- [23] M. T. Bevacqua and L. Di Donato, "Improved TV-CS approaches for inverse scattering problem," *The Scientific World Journal*, Article ID 262985, 9 pages, 2015.
- [24] O. M. Bucci, C. Gennarelli, and C. Savarese, "Representation of electromagnetic fields over arbitrary surfaces by a finite and nonredundant number of samples," *IEEE Transactions on Antennas and Propagation*, vol. 46, n. 3, pp. 351-359, 1998.
- [25] D. F. Kelley and W. L. Stutzman, "Array antenna pattern modeling methods that include mutual coupling effects," *IEEE Transactions on Antennas and Propagation*, vol. 41, n. 12, pp. 1625-1632, 1993.
- [26] C. A. Balanis, *Antenna Theory* (Third Edition), John Wiley & Sons, p. 806, 2005.
- [27] A. F. Morabito, A. Massa, P. Rocca, and T. Isernia, "An effective approach to the synthesis of phase-only reconfigurable linear arrays," *IEEE Transactions on Antennas and Propagation*, vol. 60, n. 8, pp. 3622-3631, 2012.
- [28] T. Isernia and A. F. Morabito, "Mask-constrained power synthesis of linear arrays with even excitations," *IEEE Transactions on Antennas and Propagation*, vol. 64, no. 7, pp. 3212-3217, 2016.
- [29] A. F. Morabito and P. G. Nicolaci, "Optimal synthesis of shaped beams through concentric ring isophoric sparse arrays," *IEEE Antennas and Wireless Propagation Letters*, vol. 16, pp. 979-982, 2016.

This is the post-print of the following article: R. Palmeri, T. Isernia, and A. F. Morabito, "Diagnosis of Planar Arrays through Phaseless Measurements and Sparsity Promotion," *IEEE Antennas and Wireless Propagation Letters*, vol. 18, n. 6, pp. 1273 - 1277, 2019. Article has been published in final form at: <https://ieeexplore.ieee.org/document/8704892>. DOI: 10.1109/LAWP.2019.2914529.

1536-1225 © [2019] IEEE. Personal use of this material is permitted. Permission from IEEE must be obtained for all other uses, in any current or future media, including reprinting/republishing this material for advertising or promotional purposes, creating new collective works, for resale or redistribution to servers or lists, or reuse of any copyrighted component of this work in other works."